Charge distribution, neutron evaporation, and energy distribution in higher energy binary fission

D. N. Sharma, M. R. Iyer, and A. K. Ganguly
Health Physics Division, Bhabha Atomic Research Centre, Trombay, Bombay-400085, India
(Received 6 August 1975)

A computational procedure based on the order-disorder model for predicting independent yields of fission products in higher energy fission is described. Based on the experimental observation that increase in excitation energy of the compound nucleus is used up only in exciting the fragments resulting from fission, a scheme for the distribution of extra excitation between the fragments has been evolved. The extra excitation energy is shown to be shared between the two impending fragments in proportion to the number of neutrons out of the balance number (as per the order-disorder model) going to either of the fragments. The calculational procedure essentially consists of making use of the scheme and obtaining the excitation energy of the fragments for higher energy fission from those for spontaneous fission. Data on neutrons evaporated $\bar{\nu}(Z_i, N_j)$ from individual fragments for the higher energy fission are calculated from the excitation energy using the cascade evaporation scheme. The product isotopic distributions are calculated from $\bar{\nu}(Z_i, N_j)$ data and calculated fragment isotopic distributions given by the order-disorder model. The product isotopic distributions thus calculated along with experimental product mass yield data give the independent yields of the products. The results obtained for fission of ^{235}U by fission spectrum neutrons (fast) and 14.7 MeV (high energy) neutrons are discussed in the paper. A comparison of the predicted independent yields with experimental values shows good agreement within reasonable limits. The total isotopic yield versus Z distribution for fast and high energy neutronic fission show as expected a decrease in peak to valley ratio with increasing excitation energy of the compound nucleus. $\bar{\nu}(Z_i, N_j)$ distributions for both the fission reactions are presented. They show less pronounced shell effects at $N = 50$ and 82 than in the case of thermal fission. The isotopic, isobaric, and isotonic averages of $\bar{\nu}(Z_i, N_j)$ retain the sawtooth nature as in the case of thermal fission. The Wahl plot shows that $|Z_p - Z_{UCD}|$ decreases with increasing energy of fission. The present study also confirms the experimental observation that Z_p for higher energy fission lies between the values predicted by the unchanged charge density and equal charge displacement hypotheses.

[NUCLEAR REACTIONS, FISSION ^{235}U(n,f), E=2 MeV, 14.7 MeV; calculated isotopic distributions, charge distributions, independent yields of products and neutron evaporation and energy distribution in individual fragments using order-disorder model.]

I. INTRODUCTION

Experimental studies on nuclear charge distribution in binary fission is by and large confined to thermal neutron induced (thermal fission) and spontaneous fission. Data on higher energy fission are scanty, presumably because of the relatively low fission cross sections and the resulting experimental difficulties.

Meek and Rider[1,2] have compiled radiochemical data on product mass yields and charge distribution parameters for ten fission reactions induced by neutrons in six nuclides. Product mass yields are given for masses 66 to 172. The widths (σ'_A) of Gaussian isobaric product charge distributions obtained from measured independent yields are given for 32 masses for ^{235}U thermal fission and the average value of σ'_A as 0.56 is assumed for other masses.[1] In the revised compilation,[2] however, σ'_A values have been assumed to be constant at 0.56 for all masses. No directly determined σ'_A values are available for fission spectrum neutron induced (fast) and 14.7 MeV neutron induced (HE) fission of ^{236}U. The experimental independent yield values for ^{235}U thermal, fast, and HE neutronic fissions are available for 108, 5, and 34 fission products, respectively.[2] Experimental values on cumulative yields for thermal, fast, and HE neutronic fission of ^{235}U are given for 130, 118, and 123 fission products, respectively.[2] Recommended independent and cumulative yields obtained by using isobaric charge distribution parameters are also given for all products.[2]

On the basis of the fragment formation scheme of the order-disorder model (ODM) it has been predicted that a total of 671 fission fragments in the mass range 80 to 156 are formed in fission, out of which about 333 remain to be identified.[3] Data on physical measurements of fragment mass yields are limited for higher energy fission. Even in the case of thermal fission, where many measurements exist, they suffer from limitations in mass resolution,[4] though some improved measurements are reported.[5] Charge distribution data from x-ray measurements for higher energy fission are also not readily available. Qualitative

theories on charge distribution in fission have been attempted by earlier workers,[6-12] but no satisfactory theoretical procedures to predict charge distribution parameters or independent yields in higher energy fission are available.

In the present work the ODM developed earlier[13-15] and successfully used to derive a number of parameters for thermal fission has been extended to study the charge distribution in higher energy binary fission of ^{235}U and to work out a number of connected parameters.

II. REVIEW OF THE ORDER-DISORDER MODEL

According to the ODM,[13-15] a fissioning nucleus undergoes an early charge polarization into two "impending fragments," with charges Z_L and Z_H and neutrons N_L^S and N_H^S, respectively, corresponding to the most β-stable configurations for the respective charges. This is followed by a random distribution, as in an order-disorder process, of the balance number of neutrons ($N_{bal} = 144 - N_L^S - N_H^S$, in case of ^{235}U) between the polarized impending fragments prior to scission. A schematic representation of the model is given in Fig. 1.

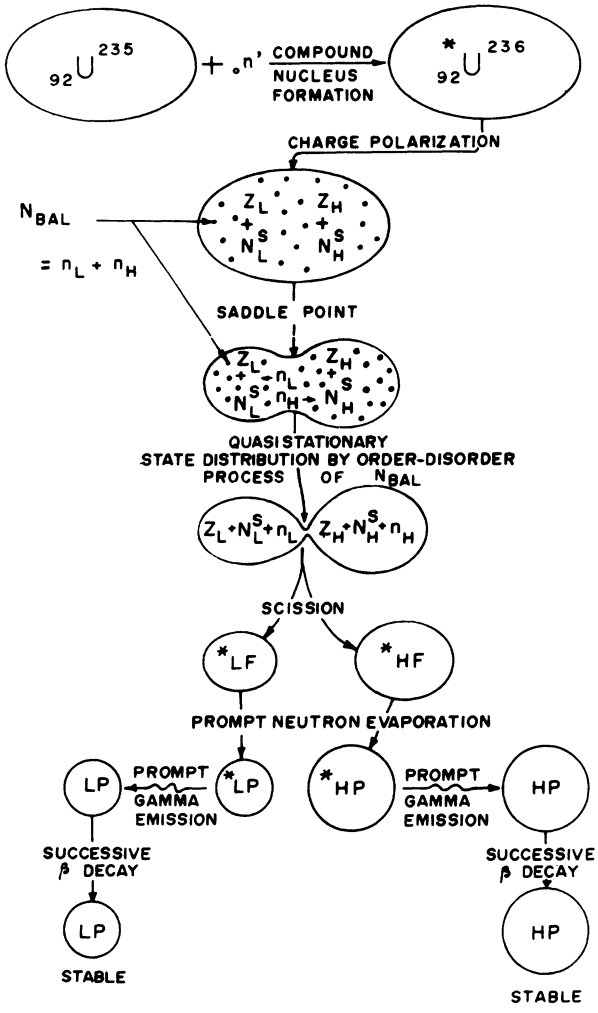

FIG. 1. The order-disorder model of fission.

A number of parameters for the thermal fission of ^{235}U have been calculated in Refs. 13–15 using the model. The procedure used in these calculations essentially consists of the following steps:

(i) Calculation of the probability distributions $P_z(Z_i, N_j)$ of fission fragments along the isotopic line (fragment isotopic distributions) of charge Z_i.

(ii) Calculation of the total isotopic yields $Y_z(Z_i)$ from fragment isotopic distributions and experimental fragment mass yields $Y_m(A_k)$ using an iterative method.

(iii) Calculation of the number of neutrons $\bar{\nu}(Z_i, N_j)$ evaporated from individual fission fragments using fragment isotopic distributions, as given by the model and those of products $P'_z(Z_i, N_j)$ calculated from published data on product mass yields $Y'_m(A_k)$ and charge distribution parameters Z'_p and σ'_A.

(iv) Calculation of the excitation energy of fission fragments from the $\bar{\nu}(Z_i, N_j)$ adopting a cascade evaporation scheme.[14]

(v) Calculation of the kinetic energy of fission fragments as the difference between fission energy and excitation energy.

The averages of the above calculated parameters along charge (isotopic), mass (isobaric), and neutron (isotonic) lines are obtained and isobaric averages are compared with available experimental data.

III. SCHEME FOR DISTRIBUTION OF EXTRA EXCITATION ENERGY BETWEEN TWO IMPENDING FRAGMENTS

The data on average number of neutrons evaporated per fission, $\bar{\nu}_T$ for neutron induced fission of ^{235}U as determined by Hopkins and Diven[16] and by Mather, Fieldhouse, and Moat,[17] show that the rate of increase of $\bar{\nu}_T$ with increasing excitation is very close to what would be expected if all the added energy is considered as extra excitation imparted to the nucleus and utilized for neutron evaporation from fragments.[18] These data cover the range of incident neutron energy from thermal to 14 MeV.

Further in support of the above, it has been observed[19-24] that in high energy fission there is very little dependence of the fragment kinetic energy on the incident neutron energy or on the excitation energy of the fissioning nucleus.

Based on these observations we adopt in the present work that the extra excitation (consisting of the binding energy of the incident neutron and its kinetic energy) imparted to the target nucleus goes into exciting the compound nucleus.

The two impending fragments consist of two β stable configurations of (Z_L, N_L^S) and (Z_H, N_H^S), leaving the balance neutrons N_{bal} to be shared among the two as in the order-disorder process. The excitation energy of fragments in spontaneous fission is then understood to be only due to the charge polarization process in the fissioning nucleus. The extra excitation of the fragments over that in the case of spontaneous fission is shared between the two fragments in proportion to the number of balance neutrons going to either of these as shown in Appendix A.

Thus, for the light fragment

$$X_{\text{th}}^L(Z_i, N_j) = X_{\text{SF}}^L(Z_i, N_j) + x_{\text{th}}(= B^C)\frac{n_L}{N_{\text{bal}}} \quad (1)$$

and

$$X_{\text{HE}}^L(Z_i, N_j) = X_{\text{SF}}^L(Z_i, N_j) + x_{\text{HE}}(= B^C + e^C)\frac{n_L}{N_{\text{bal}}} \quad (2)$$

where $X_{\text{SF}}^L(Z_i, N_j)$ is the excitation energy of a light fragment in spontaneous fission. Lower subscripts th, F, and HE indicate the parameter for thermal, fast, and high energy fissions, respectively; x_{th} is the extra excitation of the fissioning nucleus in thermal fission over that corresponding to spontaneous fission. Subscripts F and HE indicate the parameter for fast and high energy fission; B^C is the binding energy of the incident neutron to the target nucleus; e^C is the kinetic energy of the incident neutron; n_L is the number of neutrons out of N_{bal} going to the light fragment.

IV. PROCEDURE FOR CALCULATING PRODUCT INDEPENDENT YIELDS FOR FISSION OF ANY ENERGY

The computational procedure for calculating independent yields of fission products in fission of any energy consists of the following steps: (i) computation of fragment excitation energy; (ii) computation of $\bar{\nu}(Z_i, N_j)$ from these excitation energies; (iii) computation of fission product isotopic distributions from $\bar{\nu}(Z_i, N_j)$; (iv) computation of total isotopic yield vs Z distribution; (v) computation of fission product independent yields. Description of the procedure in sequence is given below.

A. Computation of fragment excitation energy

The fragment isotopic distributions obtained from ODM and the calculated product isotopic distributions (cf. Sec. II) for thermal fission are used[14] to calculate the number of neutrons $\bar{\nu}(Z_i, N_j)$ evaporated from individual fragments in thermal fission. From $\bar{\nu}(Z_i, N_j)$ data the excitation energy of individual fragments in thermal fission is calculated[14] adopting the cascade evaporation scheme. The extra excitation of a pair of fragments in thermal fission over that for spontaneous fission is the binding energy of the incident neutron in the fissioning nucleus. This extra excitation energy is shared between the two fragments as per the scheme outlined in Sec. III. Hence by subtracting the extra from the calculated excitation energy of individual fragments in thermal fission the fragment excitation energy in case of spontaneous fission is worked out.

These excitation energies for spontaneous fission are used as the base values for calculating the excitation energy of fragments for higher energy fissions as indicated in Sec. III. Due to the nonavailability of sufficient experimental data on spontaneous fission the base values could not be obtained directly.

B. Computation of $\bar{\nu}(Z_i, N_j)$

Iyer and Ganguly[14] adopted a cascade evaporation scheme to compute the excitation energy of each fragment using Weisskopf's[25] statistical model and $\bar{\nu}(Z_i, N_j)$ computed using their accounting method.[14] The scheme for obtaining the $\bar{\nu}(Z_i, N_j)$ from excitation energy of fragments in higher energy fission then consists of applying the cascade evaporation scheme in the reverse, i.e., to compute $\bar{\nu}(Z_i, N_j)$ from the computed excitation energy of the fragments using Weisskopf's statistical model. The procedure is described in Appendix B.

C. Computation of fission product isotopic distributions

The fission fragment isotopic distributions given by the ODM depend only on the β stable configurations[13] resulting from charge polarization which in turn determines the balance number of neutrons to be shared by the two impending fragments. As such these distributions remain the same for fission of any energy. The accounting method of Iyer and Ganguly[14] to calculate $\bar{\nu}(Z_i, N_j)$ from each fragment has been used in reverse to calculate fission product isotopic distributions from the fission fragment isotopic distributions (as derived in Sec. II) and $\bar{\nu}(Z_i, N_j)$ calculated in Sec. IV B. In this formulation a nonintegral number of neutrons evaporated is looked upon as the fission fragment evaporating two integral number of neutrons on either side of the nonintegral number with appropriate weights.

The product isotopic distributions $P'_z(Z_i, N_j)$ have also been calculated using Terrell's summation method[18] in reverse, using the fragment distributions and $\bar{\nu}(Z_i, N_j)$ values. The distributions obtained by the two methods agree well.

D. Computation of total isotopic yield vs Z distribution

The calculated fission product isotopic distributions and published fission product mass yields (experimental) are then used to calculate the total isotopic yield for each charge by using an iterative procedure[13] which solves the following simultaneous equations:

$$\sum_{ij} Y_z(Z_i)[P'_z(Z_i, N_j)] = Y'_m(A_k) \qquad (3)$$

with the boundary conditions

$$Z_i + N_j = A_k,$$

$$\sum_k Y'_m(A_k) = \sum_i Y_z(Z_i),$$

$$\sum_j P'_z(Z_i, N_j) = 1,$$

where $Y_z(Z_i)$ is the total isotopic yield for a charge Z_i.

E. Computation of fission product independent yields

The total isotopic yields obtained from the iterative method are multiplied by the product isotopic distributions obtained in Sec. IV C to get the independent yield of each product species.

V. INPUT DATA FOR THE CALCULATIONS

A. Data for calculation of fragment isotopic distributions

The data on the most β stable neutron number for charges are calculated from the compilation of Dewdney.[26] Dewdney has arrived at the most β stable charge for a mass from experimental β decay energies. From these the most β stable neutron number for each charge is obtained.

The mass formula used in the calculations is the one given by Zeldes, Gronau, and Lev.[27] Though Zeldes's mass formula does not have the theoretical elegance of certain others like, say, that of Myers and Swiatecki,[28] by using a large number of fitted parameters it seems to give ground state masses sufficiently accurately.

B. Data for calculation of fragment excitation energy in thermal fission

The input data required for calculation of product isotopic distributions are the product mass yields and charge distribution parameters. These are taken from the compilation of Meek and Rider.[2] In their revised compilation, however, they have given the Gaussian spread (σ'_A) as constant for all masses. As it is known that the σ'_A is a function of A,[15,29] we have used variable σ'_A compiled by Meek and Rider in their earlier compilation.[1] In the region where no experimental values were available the linearly interpolated values were used.

The consistency and accuracy of input data on fission product mass yields and charge distribution parameters in thermal fission which are used as input do influence the accuracy of predicted parameters for higher energy fissions. The latest and most consistent data have been used in these computations. Based on the necessary condition of equality of complementary charge yields,[13] a procedure has been developed to evaluate a set of mass yields and charge distribution parameters. These studies show that the latest set of Meek and Rider data also does not satisfy this condition.

$\bar{\nu}(Z_i, N_j)$ values obtained from fragment and product isotopic distributions have been used to calculate the excitation energy of fragments using the cascade evaporation scheme given in Ref. 14. Zeldes's mass formula has been used in these calculations. The temperature parameter used in these calculations is taken from Gilbert and Cameron.[30]

C. Data for calculation of product isotopic distributions for higher energy fission

The binding energy of the neutron to the ^{235}U nucleus is taken as 6.5 MeV. For obtaining neutron binding energies in these calculations, Zeldes's mass formula is used.

D. Data for the calculation of total isotopic yield distribution for higher energy fission

The computation of total isotopic yields from the product isotopic distributions using the iterative method involves the use of experimental fission product mass yield data for the particular fission reaction. These data are taken from Meek and Rider.[2] The errors quoted for mass yields by Meek and Rider are used to calculate errors in total isotopic yields.

VI. RESULTS AND DISCUSSION

A. Fission product isotopic distributions

Fission product isotopic distributions for $Z = 28$ to 64 have been computed for the fast and HE fission of ^{235}U using the procedure indicated in Sec. IV and the data of Sec. V. The distributions were

all single peaked functions but were not amenable to good fitting with a Gaussian distribution.

The calculation of fission product isotopic distributions for higher energy fission starting from the fission fragment isotopic distribution for a typical case $Z = 41$ is shown in Figs. 2(a)–2(d).

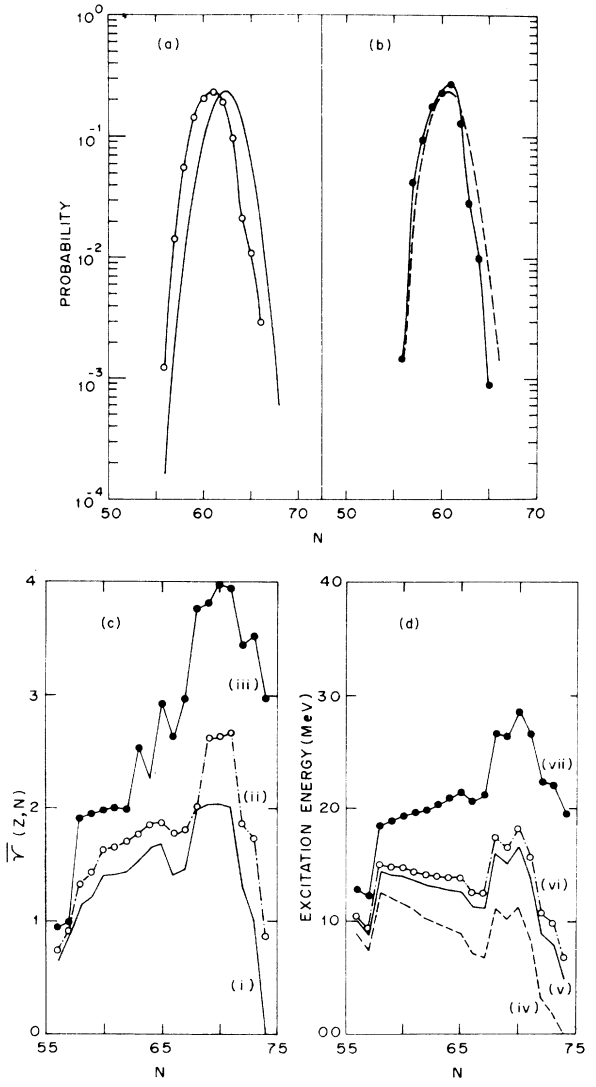

FIG. 2. Calculation of fission product isotopic distribution for HE fission for a typical case of $Z = 41$. (a) shows the fragment (——) and product (○—○) isotopic distribution from which $\bar{\nu}(Z,N)$ for thermal fission is calculated [curve (i) in (c)]. Curves (v), (iv), (vi), and (vii) in (d) show excitation energies of fragments for thermal, spontaneous, fast, and HE fission, respectively, calculated therefrom. From these, $\bar{\nu}(Z,N)$ for fast and HE fission are obtained [curves (ii) and (iii), respectively, in (c)]. (b) shows the calculated product isotopic distribution for fast (---) and HE (●—●) fission using the fragment isotopic distribution [in (a)] and $\bar{\nu}(Z,N)$ for the respective cases [curves (ii) and (iii), respectively, in (c)].

Figure 2(a) shows the fragment isotopic distribution from the ODM and the fission product isotopic distribution for thermal fission calculated from published experimental data (Sec. V). The $\bar{\nu}(Z_i,N_j)$ distribution obtained therefrom for thermal fission using the accounting method is shown in Fig. 2(c). The excitation energy calculated from this $\bar{\nu}(Z_i,N_j)$ using the cascade evaporation scheme is shown in Fig. 2(d). The base values for excitation energy corresponding to spontaneous fission calculated from this using the scheme for division of extra excitation energy is also shown in Fig. 2(d). The excitation energies for fast and HE fission calculated therefrom are indicated in Fig. 2(d). Employing the evaporation scheme in reverse (Sec. IV B), the $\bar{\nu}(Z_i,N_j)$ obtained for fast and HE fission are also presented in Fig. 2(c). The fission product isotopic distributions for fast and HE fission obtained from fission fragment isotopic distributions and $\bar{\nu}(Z_i,N_j)$ for the respective cases by applying the accounting procedure in reverse are shown in Fig. 2(b).

A new parameter for representing the mean neutron number for isotopic distributions as a function of Z has been adopted. The difference of the mean neutron number of fragment isotopic distributions (N_p) from neutron number corresponding to unchanged neutron density for fragments ($N_{UND} = \frac{144}{92}Z$ for neutronic fission of ^{235}U) is plotted as a function of Z. N'_{UND} for product isotopic distributions is obtained by correcting N'_{UND} for $\bar{\nu}(Z)$. The parameter $(N'_{UND} - N'_p)$, where N'_p is the mean neutron number of product isotopic

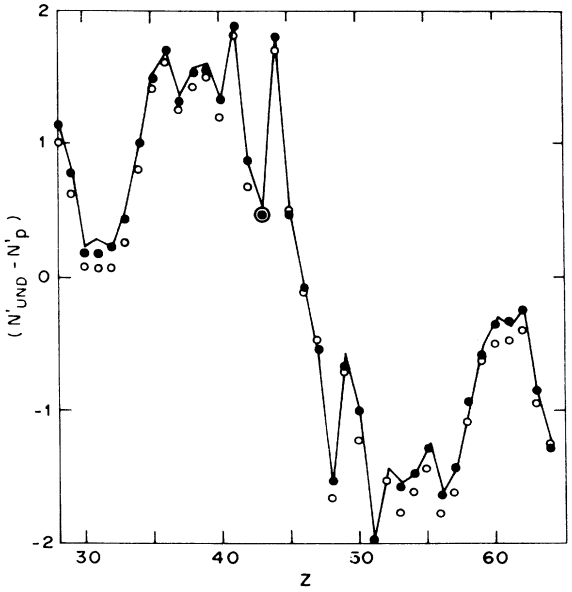

FIG. 3. $(N'_{UND} - N'_p)$ versus Z for thermal (——), fast (●), and HE (○) fission of ^{235}U.

distribution, is plotted as a function of Z. The plots for thermal, fast, and HE fission of ^{235}U are given in Fig. 3. The results show that this function decreases with increasing excitation energy of the compound nucleus. Similar functions can be used to study isotopic distribution of fragments also.

B. Total isotopic yield vs Z distribution

The total isotopic yields obtained using the iterative procedure of Sec. IV and using the data of Sec. V for fast and HE fissions of ^{235}U are shown in Figs. 4(a) and 5(a), respectively. The transmission of errors from the product mass yield data to the computed values of total isotopic yields is obtained by using the errors in product mass yields as the input for the iterative procedure. The errors so obtained are shown in Figs. 4(a) and 5(a).

The total isotopic yield should be the same for complementary charges whether it is for fragments or for products. This is because neutron evaporation does not change the charge of the species and they continue to be in the same isotopic line even after neutron evaporation. The equality of complementary charge yields is a necessary condition. The calculated total isotopic yields for fast and HE fission are not found to exactly satisfy this condition. This could be caused by (a) experimental errors in the input product mass yields and/or (b) errors in product isotopic distributions reflected from input data on charge distribution and mass yields for thermal fission used in the calculations (Sec. II). In most of the cases it is observed that the reflected point of the higher Z yields lies within the standard deviation of the complementary lighter Z yields. We look upon these yield values as obtained from two different sets of values for a given charge pair and hence the mean of these two has been used as the accepted value for the charge pair. The accepted total isotopic yields are shown in Fig. 4(b) and 5(b) for fast and HE fission of ^{235}U, respectively.

The peak to valley ratios of the total isotopic yield distribution for the fast and HE fission of ^{235}U obtained in the present work are 214 and 5, respectively, and they compare well with 220 and 6 as given by the experimental fission product mass yield data.[2]

C. Fission product independent yields

The accepted total isotopic yield distribution when multiplied with product isotopic distributions gives independent yields for products.

As has been reviewed earlier, Meek and Rider[2] have compiled direct experimental independent yields for five fission products and direct experimental cumulative yields for 118 fission products in fast fission. The number of measurements available for independent and cumulative yields for HE fission are 34 and 123, respectively.

The experimental and the predicted values of independent and cumulative yields in the present work do not agree very well in all cases. Generally speaking the agreement seems to be better

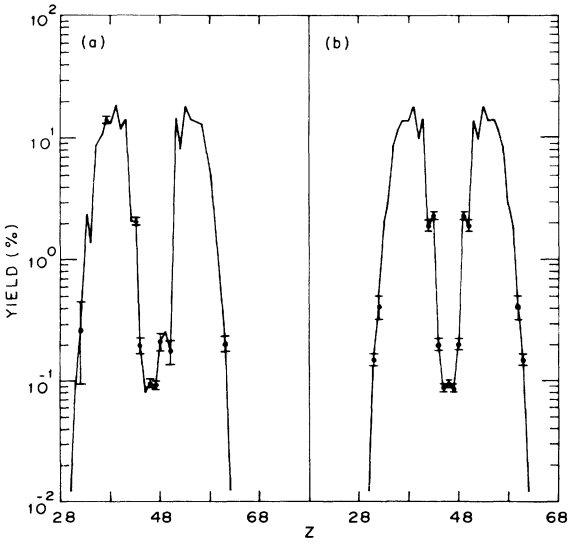

FIG. 4. The total isotopic yields for $^{235}U(n_F,F)$. (a) shows the output using the iterative procedure, and (b) shows the accepted solution.

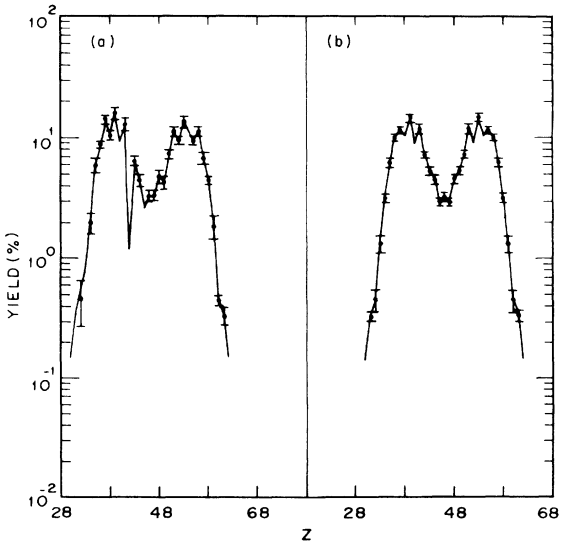

FIG. 5. The total isotopic yields for $^{235}U(n_{HE},F)$. (a) shows the output using the iterative procedure, and (b) shows the accepted solution.

TABLE I. Distribution of the predicted independent and cumulative yield values with respect to deviation with the experimental values.

Difference of the predicted and experimental values lying between	Independent yields		Cumulative yields	
	Fast	HE	Fast	HE
0 and σ	...	6	6	5
σ and 2σ	1	6	2	2
2σ and 3σ	...	4	3	6
3σ and 4σ	1	2	...	5
4σ and 5σ	...	...	1	3
$>5\sigma$	1	8	4	4

in the higher yield region. It has not been possible to resolve all these differences. In certain cases even the experimental values quoted in the 1972 compilation of Meek and Rider differ by a factor of 2 from the 1974 values. Considering the large variation in recommended values given by Meek and Rider and the range of experimental uncertainties quoted for experimental values, it can be stated that the present approach predicts the independent and cumulative yields within reasonable limits of errors. However, in case of isomeric transitions the present approach cannot differentiate between ground and metastable states and predicts a single value for each product species. As such, comparison with the experimental values is made in those cases where only the ground state products exist. Table I shows the distribution of yield predictions having various degrees of differences (in terms of given standard deviations) with experimental values.

D. Charge distribution parameters

The nuclear charge distribution in fission is usually discussed in terms of charge dispersion

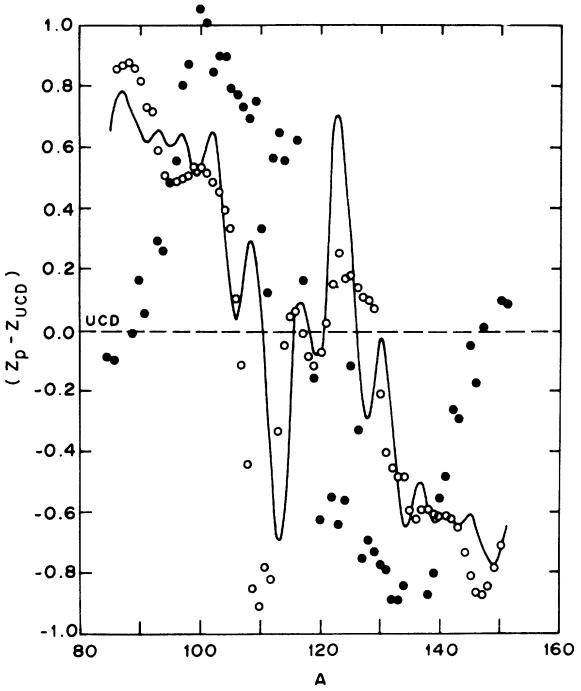

FIG. 6. $(Z_p - Z_{UCD})$ versus A for fragments from $^{235}U(n_F, F)$ obtained in the present work (—) is compared with that calculated using published Z'_p values (○) (Ref. 2) for fast fission changed to fragment mass using $\bar{\nu}(A)$ obtained in the present work. (●) and (---) give the Wahl plot obtained using Z_p values, corresponding to the ECD and UCD hypotheses, respectively.

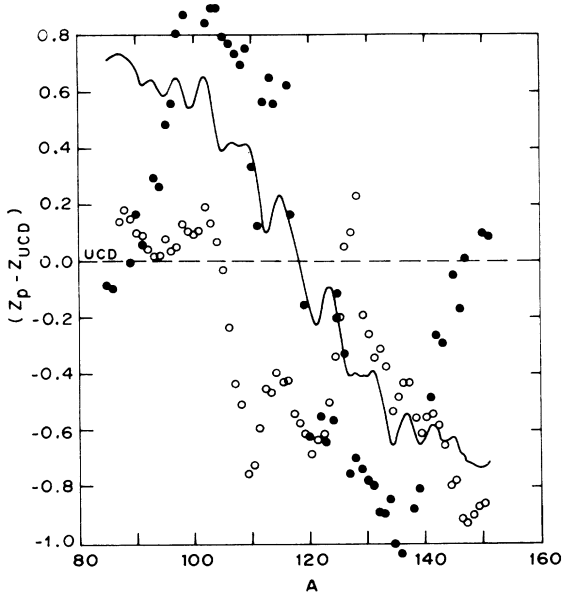

FIG. 7. $(Z_p - Z_{UCD})$ versus A for fragments from $^{235}U(n_{HE}, F)$ obtained in the present work (——) is compared with that calculated using Z'_p values (○) (Ref. 2) for HE fission changed to fragment mass using $\bar{\nu}(A)$ obtained in the present work. (●) and (---) give the Wahl plot obtained using Z_p values corresponding to the ECD and UCD hypotheses, respectively.

in primary fission products with the same mass number. The isobaric charge distributions are conventionally fitted to a Gaussian of the form

$$(C_A\pi)^{-1/2}\exp[-(Z-Z_p)^2/C_A], \tag{4}$$

where

$$C_A = 2(\sigma_A{}^2 + \tfrac{1}{12}). \tag{5}$$

The distributions obtained in the present work confirm the conclusions of Wahl *et al.*[29] that they are not exactly Gaussian. They have asymmetry and structures in them. The mean of the charge distribution is, however, independent of the assumption of Gaussian distribution. The mean Z_p of product and fragment isobaric charge distributions has been worked out for masses 85 to 156 for fast and HE fissions of ^{235}U. The parameter $(Z_p - Z_{\mathrm{UCD}})$, where $Z_{\mathrm{UCD}} = (\frac{92}{236})A$, for fragments is plotted as a function of fragment mass (Wahl plot) for the two fission reactions in Figs. 6 and 7. The Z_p tabulated by Meek and Rider[2] are for products and they are plotted as $(Z_p - Z_{\mathrm{UCD}})$ in Figs. 6 and 7 after correcting the product masses by $\bar{\nu}(A_k)$ obtained in the present work for the sake of comparison. $(Z_p - Z_{\mathrm{UCD}})$ values obtained using the equal charge displacement (ECD) hypothesis are also shown. In order to conserve the charge of the fissioning nucleus, $(Z_p - Z_{\mathrm{UCD}})$ for two complementary fragments should be equal in value but opposite in sign. The values obtained using the Meek and Rider[2] data on charge distribution do not satisfy this condition in either case, but the agreement is worse in HE fission. An evaluation study of the Meek-Rider data on charge distribution parameters and product mass yields for fast and HE fission of ^{235}U shows that they do not form a consistent set from the point of view of equality of complementary charge yields.

Many experiments[31-33] have concluded that Z_p for higher energy fission lies between ECD and unchanged charge density (UCD). This seems to be true in the present work also at least for the high yield region. Further, the present study also shows that $|Z_p - Z_{\mathrm{UCD}}|$ decreases with increasing energy of fission.

E. Number of neutrons evaporated from individual fragments $\bar{\nu}(Z_i, N_j)$

$\bar{\nu}(Z_i, N_j)$ for charges $Z = 28$ to 64 worked out using the procedure of Sec. IV are presented as functions of N for each Z in Figs. 8 and 9 for fast and HE fission, respectively. The effects of neutron magic numbers on $\bar{\nu}(Z_i, N_j)$, though discernible, are not that pronounced as in the case of thermal fission (cf. Ref. 14). The measurement

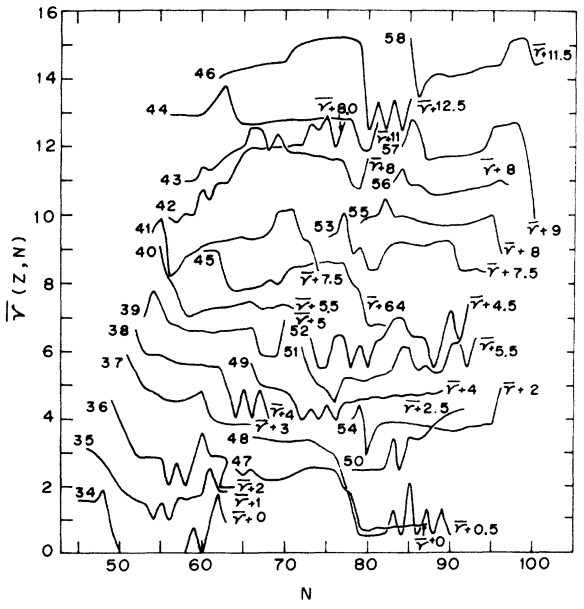

FIG. 8. Number of neutrons $\bar{\nu}(Z,N)$ emitted by individual fragments in fast fission of ^{235}U as functions of the neutron number N of the fragment for $Z = 34$ to 58. The $\bar{\nu}$ axis is shifted by the number indicated for each curve (on the right) to avoid crowding. The number on the left of each curve indicates the Z of the fragments.

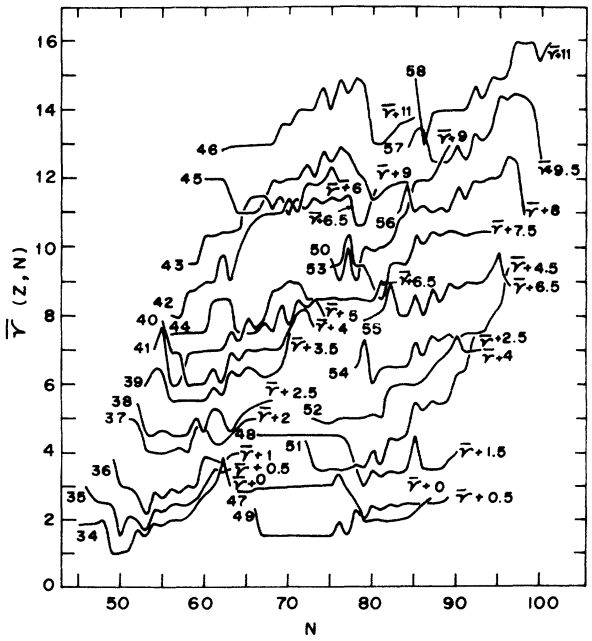

FIG. 9. Number of neutrons $\bar{\nu}(Z,N)$ emitted by individual fragments in HE fission of ^{235}U as functions of the neutron number N of the fragment for $Z = 34$ to 58. The $\bar{\nu}$ axis is shifted by the number indicated for each curve (on the right) to avoid crowding. The number on the left of each curve indicates the Z of the fragments.

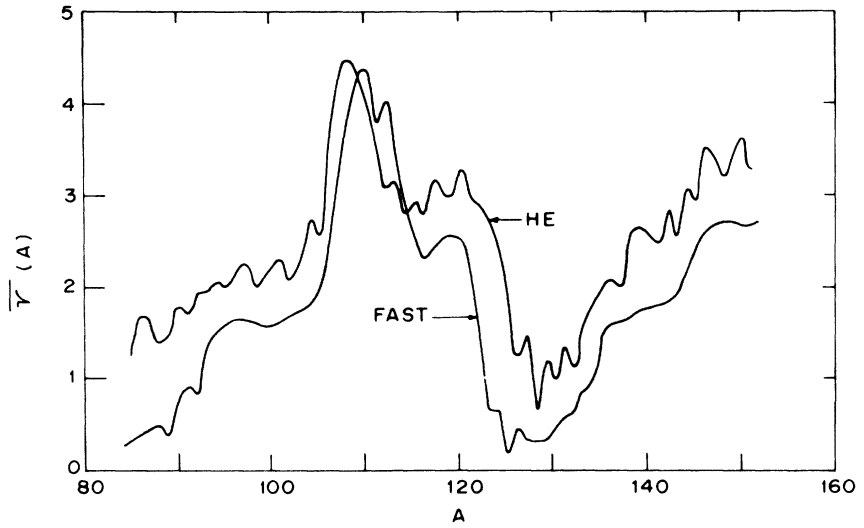

FIG. 10. $\overline{\nu}$ (A) versus A for single fragments for the fast and HE fission of ^{235}U.

of $\overline{\nu}(Z_i, N_j)$ parameters involves the detection of neutrons from an individual fragment characterized by a single mass and charge. Even for the relatively simpler case of thermal fission it has not been possible to measure them.

The $\overline{\nu}(Z_i, N_j)$ values along with the absolute yield of fragments obtained earlier are used to get isobaric $\overline{\nu}(A_k)$, isotopic $\overline{\nu}(Z_i)$, and isotonic $\overline{\nu}(N_j)$ averages. They are shown in Figs. 10–12 for the two fission reactions. We have not come across any measurement of $\overline{\nu}(A_k)$ for higher energy fission and hence it has not been possible to compare the present result with experimental values. However, the sawtooth nature of the distribution seen in the thermal fission case[14] is retained here. The effect of proton magic numbers $Z = 28$ and 50 and the effect of neutron magic numbers $N = 50$ and 82 are seen in the $\overline{\nu}(Z_i)$ and $\overline{\nu}(N_j)$ distributions, respectively, both for fast and HE fission of ^{235}U, though the effect seems to be slightly less in the latter case.

The integration of $\overline{\nu}(A_k)$ over the totality of fission fragments give the total neutrons $\overline{\nu}_T$ evaporated in fission. The computed value of $\overline{\nu}_T$ for fast fission comes to 3.21 which is higher than the reported value 2.65,[18] but the value for HE comes to 4.86, which is comparable to the reported value of 4.65,[18] within experimental uncertainty. In the case of fast fission the approximation of fission spectrum neutron fission to 2.0 MeV neutronic fission may yield a higher value of $\overline{\nu}_T$ for fast fission.

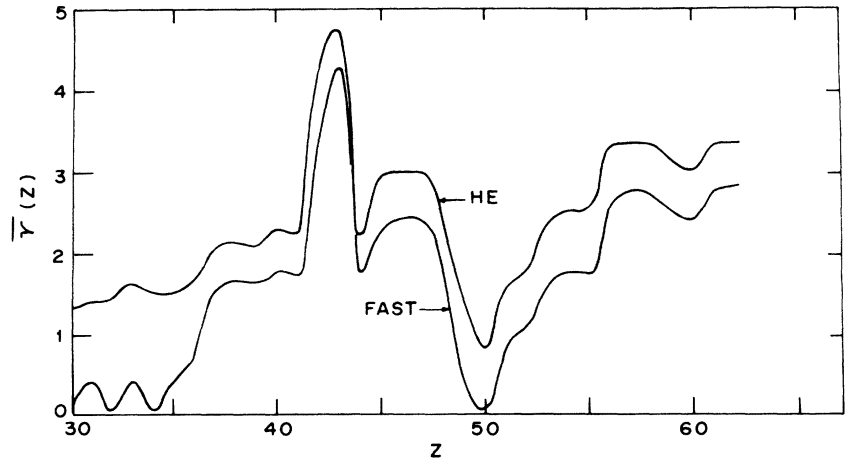

FIG. 11. $\overline{\nu}$ (Z) versus Z for single fragments for the fast and HE fission of ^{235}U.

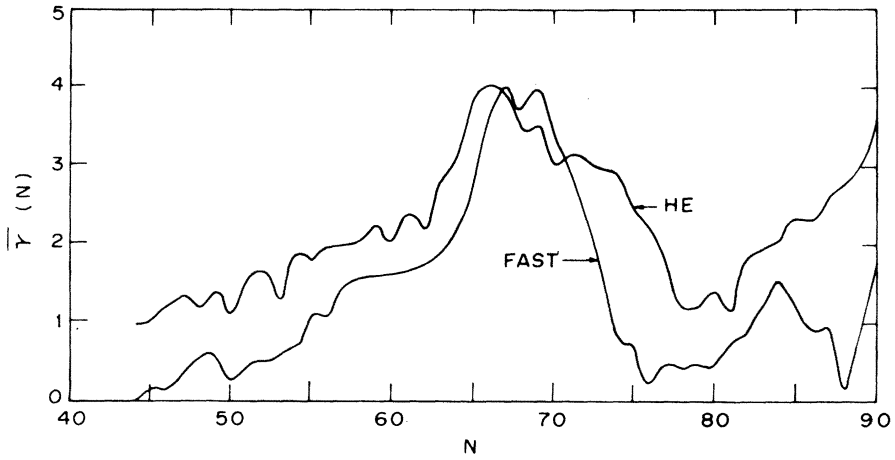

FIG. 12. $\bar{\nu}(N)$ versus N for single fragments for the fast and HE fission of ^{235}U.

F. Variation of $\bar{\nu}(Z_i)$ with excitation energy

As can be seen from the description of the procedure (Sec. IV), the computation of $\bar{\nu}(Z_i, N_j)$ for fission with any energy of incident neutron can be obtained from the base values of fragment excitation energy corresponding to spontaneous fission without any additional input data. This, along with the fragment isotopic distributions, enables one to calculate $\bar{\nu}(Z_i)$ for any given higher energy fission. The $\bar{\nu}(Z_i)$ values so worked out at an interval of 2 MeV from 0 to 14.7 MeV are shown in Fig. 13 as a function of the compound nucleus excitation energy for each Z. The results for pairs of charge are given in Fig. 14.

In the present work the $\bar{\nu}_T$ for each discrete energy fission could not be obtained as this needs total isotopic yields involving the use of input product mass yield data which are not readily available. Because of this it has been possible to calculate only for fast and HE fission of ^{235}U. Using the $\bar{\nu}_T$ for fast and HE fission obtained in the present work we get a $d\bar{\nu}_T/dE$ of 0.13. Terrell[18] obtained a value of 0.16 for the same energy range.

APPENDIX A: DISTRIBUTION OF EXTRA EXCITATION BETWEEN TWO IMPENDING FRAGMENTS

As envisaged in the ODM, the fissioning nucleus after charge polarization proceeds through quasi-stationary states and the balance neutrons N_{bal} are considered as free Fermi gas particles. Let n_L and n_H be the number of neutrons out of N_{bal} assigned to the lower and higher charge impending fragments, respectively. If V_L and V_H are the volumes of the light and heavy fragments such that $V_L + V_H = V$, the volume of the compound nucleus, then the volumes available for n_L and n_H are V_L and V_H, respectively. The Fermi gas pressure for these two fragments P_L and P_H are equal to the total Fermi gas pressure P and the temperatures of the two impending fragments are also the same at the point of scission. The energy E_L of a Fermi gas comprising of n_L particles in volume V_L at temperature kT_L is given by[34]

$$E_L = \tfrac{3}{5} n_L \frac{h^2}{2m}\left(\frac{3n_L}{8\pi V_L}\right)^{2/3} \times\left[1+\tfrac{5}{12}(kT_L)^2\frac{4\pi^2 m^2}{h^4}\left(\frac{8\pi V_L}{3n_L}\right)^{4/3}-\cdots\right], \tag{6}$$

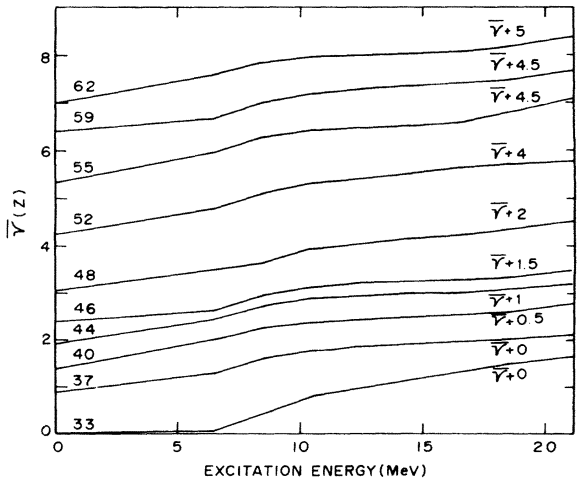

FIG. 13. The variation of $\bar{\nu}(Z)$ for some charges as a function of the excitation of the fissioning nucleus for the neutronic fission of ^{235}U. The $\bar{\nu}(Z)$ axis is shifted by the number indicated on the right and the charge number is indicated on the left of each curve.

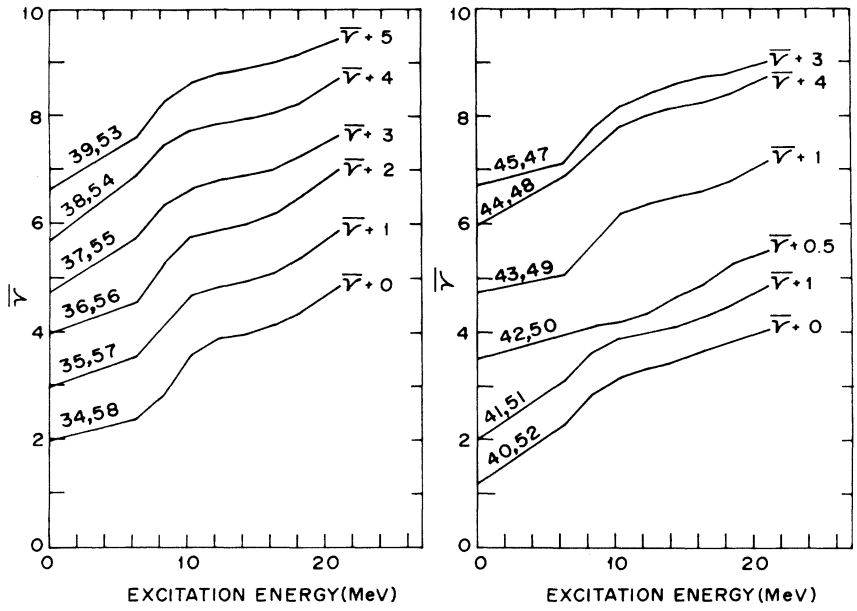

FIG. 14. The variation of $\bar{\nu}$ (Z) for complementary charge pairs as a function of the excitation of the fissioning nucleus for the neutronic fission of ^{235}U. The $\bar{\nu}$ (Z) axis is shifted by the number indicated on the right and the charge of the pair is indicated on the left of each curve.

i.e.,

$$E_L = n_L \phi\left(\frac{n_L}{V_L}, kT_L\right). \tag{7}$$

As Fermi gas pressure

$$P = \frac{2}{3}\frac{E}{V}, \tag{8}$$

$$P_L = \phi\left(\frac{n_L}{V_L}, kT_L\right), \tag{9}$$

and similarly

$$P_H = \phi\left(\frac{n_H}{V_H}, kT_H\right). \tag{10}$$

At the quasistationary state $kT_L = kT_H$ and $P_L = P_H = P$, hence

$$\frac{n_L}{V_L} = \frac{n_H}{V_H} = \frac{N_{\text{bal}}}{V}. \tag{11}$$

Since N_{bal}/V is constant for a given charge polarization we have

$$E_L \propto n_L \tag{12}$$

and similarly

$$E_H \propto n_H. \tag{13}$$

Thus the extra excitation energy is shared between the two impending fragments as proportional to the balance number of neutrons going to the light and heavy fragments, respectively.

APPENDIX B: COMPUTATION OF $\bar{\nu}(Z_i, N_j)$ FROM EXCITATION ENERGY

In principle the initial excitation energy of a fragment X_1 can be related to the number of neutrons evaporated $\bar{\nu}(Z_i, N_j)$ through a multifold integral in the cascade evaporation scheme.[14] In this scheme each evaporation step leaves the nucleus with a spectrum of residual excitation energies and of these only those events which leave the nucleus with excitation energy higher than the binding energy of the last neutron in the residual nucleus can evaporate another neutron. As shown in Ref. 14, within a reasonable limit of accuracy it can be assumed that up to the penultimate step almost all the events leave the nucleus sufficiently excited to evaporate another neutron, i.e., for each evaporation step up to the penultimate one, the area under the $dn(e)/de$ vs e (e being the kinetic energy of the evaporated neutron) curve up to the cutoff energy can be normalized to unity. Hence the average energy of the evaporated neutron at each of these evaporation steps can be taken as $2kT$. Using this, the condition relating excitation energy X_n and binding energy B_N of the last neutron in the nth evaporation step can be worked out to calculate the number of neutrons $\bar{\nu}(Z_i, N_j)$ evaporated by a fragment with a given excitation energy.

The statistical model developed by Weisskopf[25] gives the energy distribution of neutrons emitted by an excited nucleus as

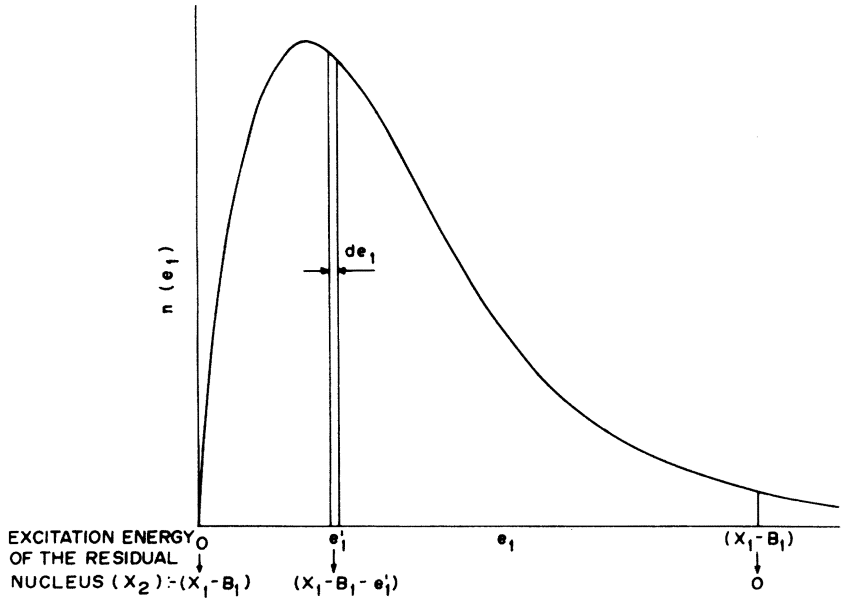

FIG. 15. Schematic diagram of the energy spectrum of the emitted neutron.

$$\frac{dn(e_1)}{de_1} \propto e_1 \exp[-e_1/kT_1], \tag{14}$$

where e_1 is the kinetic energy of the neutron emitted from a fragment with an excitation energy X_1, kT_1 is the nuclear temperature of the fragment at an excitation X_1 evaluated at its maximum residual excitation $(X_1 - B_1)$, and E_1 is the binding energy of the evaporating neutron. The kinetic energy cutoff for the emitted neutron in the first evaporation is $(X_1 - B_1)$. Equation (14) can be rewritten as

$$\frac{dn(e_1)}{de_1} = H_1 e_1 \exp[-e_1/kT_1], \tag{15}$$

where

$$0 \leq e_1 \leq X_1 - B_1,$$

$$H_1 = 1/(kT_1)^2[1 - (1+p_1)e^{-p_1}],$$

$$p_1 = (X_1 - B_1)/kT_1,$$

$$kT_1 = 1/[(a_1/U_1)^{1/2} - 1.5/U_1],$$

$$U_1 = X_1 - P(Z) - P(N).$$

H_1 is the normalization factor to give the total number of neutrons evaporated up to the cutoff energy as unity, a_1 is the nuclear temperature parameter in the level density formula,[30] and $P(Z)$ and $P(N)$ are the pairing energies.

The schematic diagram of the spectrum of energy of the emitted neutron in the first evaporation and that of the excitation in the residual nucleus is shown in Fig. 15. If the fragment excitation energy is enough only to evaporate a maximum of one neutron only, then the area under the kinetic energy curve up to infinity can be normalized to unity. The fractional area up to $(X_1 - B_1)$ will give the fraction I_1 of neutrons evaporated in the first evaporation, i.e.,

$$I_1 = \int_0^{X_1 - B_1} (kT_1)^{-2} e_1 \exp[-e_1/kT_1] de_1, \tag{16}$$

i.e.,

$$I_1 = 1 - (1+p_1)e^{-p_1}. \tag{17}$$

Thus for $I_1 > 0$ $(\bar{\nu} > 0)$, X_1 should be more than B_1. The first evaporation event leaves the nucleus with a residual excitation energy spectrum given by

$$X_2 = X_1 - B_1 - e_1 \quad \text{(cf. Fig. 15)}.$$

If B_2 is the binding energy of the last neutron in this residual nucleus then for the second evaporation event

$$X_2 > B_2$$

and

$$e_1 \leq (X_1 - B_1 - B_2).$$

This shows that only those first events which are up to kinetic energy cutoff $(X_1 - B_1 - B_2)$ will evaporate a second neutron. Thus if $X_1 \leq (B_1 + B_2)$, then $\bar{\nu} \leq 1$. If $1 < \bar{\nu} \leq 2$, the area under the kinetic energy spectrum for the first evaporation up to $(X_1 - B_1)$ can be normalized to unity. Then the area under the curve from 0 to $(X_1 - B_1 - B_2)$ will be equal to the fraction I_2 of neutrons evaporated in the second evaporation step and is given by

$$I_2 = \frac{1-\exp[-(X_1-B_1-B_2)/kT_1][1+(X_1-B_1-B_2)/kT_1]}{1-\exp[-(X_1-B_1)/kT_1][1+(X_1-B_1)/kT_1]}, \tag{18}$$

and total $\bar{\nu}$ up to the second evaporation is given by $\bar{\nu}=1+I_2$. Combining the conditions for $\bar{\nu}>0$ and $\bar{\nu}\leq 1$, the condition for $0<\bar{\nu}\leq 1$ will be

$$B_1 < X_1 \leq (B_1+B_2).$$

Similarly, it can be shown that for $1<\bar{\nu}\leq 2$ the condition will be

$$B_2 < X_2 \leq (B_2+B_3),$$

and in general for $(n-1)<\bar{\nu}\leq n$,

$$B_n < X_n \leq (B_n+B_{n+1}).$$

The total $\bar{\nu}$ for the nth evaporation is given by

$$\bar{\nu}=(n-1)+I_n,$$

where

$$I_n = \frac{1-\exp[-(X_{n-1}-B_{n-1}-B_n)/kT_{n-1}][1+(X_{n-1}-B_{n-1}-B_n)/kT_{n-1}]}{1-\exp[-(X_{n-1}-B_{n-1})/kT_{n-1}][1+(X_{n-1}-B_{n-1})/kT_{n-1}]}. \tag{19}$$

With these conditions applied to the calculated excitation energy for each fragment, the integral part of $\bar{\nu}(Z_i, N_j)$ can be determined and then the fractional part can be calculated as outlined above.

[1]M. E. Meek and B. F. Rider, General Electric Company, Vallecitos Nuclear Center, Pleasanton, California, Report No. NEDO-12154, 1972 (unpublished).

[2]M. E. Meek and B. F. Rider, General Electric Company, Vallecitos Nuclear Center, Pleasanton, California, Report No. NEDO-12154-1, 1974 (unpublished).

[3]M. R. Iyer, D. N. Sharma, and A. K. Ganguly, in Proceedings of the International Atomic Energy Agency Meeting on Fission Product Nuclear Data, Bologna, Italy, November 26–30, 1973, Vol. II, p. 29.

[4]A. C. Pappas, J. Alastad, and E. Hagebo, in *Proceedings of the Second Symposium on the Physics and Chemistry of Fission, Vienna, Austria, 1969* (International Atomic Energy Agency, Vienna, Austria, 1969), p. 669.

[5]J. P. Unik, J. E. Gindler, L. E. Glendenin, K. F. Flynn, A. Gorski, and R. K. Sjoblom, in *Proceedings of the Third International Atomic Energy Symposium on the Physics and Chemistry of Fission, Rochester, 1973* (International Atomic Energy Agency, Vienna, Austria, 1974), Vol. II, p. 19.

[6]R. Ramanna, R. Subramanian, and R. N. Aiyer, Nucl. Phys. 67, 529 (1965).

[7]V. S. Ramamurthy and R. Ramanna, in *Proceedings of the Second Symposium on the Physics and Chemistry of Fission, Vienna, Austria, 1969* (see Ref. 4), p. 41.

[8]W. Norenberg, Z. Phys. 197, 246 (1966).

[9]P. Fong, Phys. Rev. 102, 434 (1956).

[10]H. W. Newson, Phys. Rev. 122, 1224 (1961).

[11]H. Faissner and K. Wildermuth, Phys. Rev. 58, 177 (1964).

[12]H. Faissner, Z. Naturforsch 21A, 1021 (1966).

[13]M. R. Iyer and A. K. Ganguly, Phys. Rev. C 3, 785 (1971).

[14]M. R. Iyer and A. K. Ganguly, Phys. Rev. C 5, 1410 (1972).

[15]M. R. Iyer, Ph.D. thesis, Gujarat University, India, 1971 (unpublished).

[16]J. C. Hopkins and B. C. Diven, Nucl. Phys. 48, 433 (1963).

[17]D. S. Mather, P. Fieldhouse, and A. Moat, Phys. Rev. 133B, 1403 (1964).

[18]J. Terrell, in *Proceedings of the First Symposium on the Physics and Chemistry of Fission, Salzburg, 1965* (International Atomic Energy Agency, Vienna, Austria, 1965), Vol. II, p. 3.

[19]G. Friedlander, in *Proceedings of the First Symposium on the Physics and Chemistry of Fission, Salzburg, 1965* (see Ref. 18), Vol. II, p. 265.

[20]G. E. Gordon, A. E. Larsh, and T. Sikkeland, University of California Report No. UCRL-9003, 1959 (unpublished).

[21]E. K. Hyde, University of California Report No. UCRL-9065, 1960 (unpublished).

[22]E. M. Douthett and D. H. Templeton, Phys. Rev. 94, 128 (1954).

[23]G. F. Denisenko, N. S. Ivanova, N. R. Novikova, N. A. Perfilov, E. I. Prokoffieva, and V. P. Shamov, Phys. Rev. 109, 1779 (1958).

[24]E. Konecny, H. J. Specht, and J. Weber, in *Proceedings of the Third Symposium on the Physics and Chemistry of Fission, Rochester, 1973* (see Ref. 5), Vol. II, p. 3.

[25]J. M. Blatt and V. F. Weisskopf, *Theoretical Nuclear Physics* (Wiley, New York, 1956).

[26]J. W. Dewdney, Nucl. Phys. 43, 303 (1963).

[27]N. Zeldes, M. Gronau, and A. Lev, Nucl. Phys. 63, 1 (1965).

[28]W. D. Myers and W. J. Swiatecki, University of California Report No. UCRL-11980, 1965 (unpublished).

[29]A. C. Wahl, A. E. Norris, R. A. Rouse, and J. C. Williams, in *Proceedings of the Second Symposium on the Physics and Chemistry of Fission, Vienna, Austria, 1969* (see Ref. 4), p. 813.

[30]A. Gilbert and A. G. W. Cameron, Can. J. Phys. 43, 1446 (1965).
[31]W. M. Gibson, University of California Report No. UCRL-3493, 1956 (unpublished).
[32]H. Umesawa, in *Proceedings of the Second Symposium on the Physics and Chemistry of Fission, Vienna, Austria, 1969* (see Ref. 4), p. 942.
[33]S. R. Rao, Ph.D. thesis, University of Arkansas, 1973 (unpublished).
[34]S. Glasstone, *Theoretical Chemistry* (Van Nostrand, Princeton, New Jersey, New York, 1958).